

Spreading of diseases through comorbidity networks across life and gender

This content has been downloaded from IOPscience. Please scroll down to see the full text.

2014 New J. Phys. 16 115013

(<http://iopscience.iop.org/1367-2630/16/11/115013>)

View [the table of contents for this issue](#), or go to the [journal homepage](#) for more

Download details:

IP Address: 147.125.65.186

This content was downloaded on 26/02/2016 at 10:32

Please note that [terms and conditions apply](#).

Spreading of diseases through comorbidity networks across life and gender

Anna Chmiel¹, Peter Klimek¹ and Stefan Thurner^{1,2,3}

¹ Section for Science of Complex Systems, CeMSIIS, Medical University of Vienna, Spitalgasse 23, A-1090, Austria

² Santa Fe Institute, 1399 Hyde Park Road, Santa Fe, NM 87501, USA

³ IIASA, Schlossplatz 1, A-2361 Laxenburg, Austria

E-mail: stefan.thurner@meduniwien.ac.at

Received 16 May 2014, revised 15 September 2014

Accepted for publication 9 October 2014

Published 14 November 2014

New Journal of Physics **16** (2014) 115013

doi:[10.1088/1367-2630/16/11/115013](https://doi.org/10.1088/1367-2630/16/11/115013)


Abstract

The state of health of patients is typically not characterized by a single disease alone but by multiple (comorbid) medical conditions. These comorbidities may depend strongly on age and gender. We propose a specific phenomenological comorbidity network of human diseases that is based on medical claims data of the entire population of Austria. The network is constructed from a two-layer multiplex network, where in one layer the links represent the conditional probability for a comorbidity, and in the other the links contain the respective statistical significance. We show that the network undergoes dramatic structural changes across the lifetime of patients. Disease networks for children consist of a single, strongly interconnected cluster. During adolescence and adulthood further disease clusters emerge that are related to specific classes of diseases, such as circulatory, mental, or genitourinary disorders. For people over 65 these clusters start to merge, and highly connected hubs dominate the network. These hubs are related to hypertension, chronic ischemic heart diseases, and chronic obstructive pulmonary diseases. We introduce a simple diffusion model to understand the spreading of diseases on the disease network at the population level. For the first time we are able to show that patients predominantly develop diseases that are in close network proximity to disorders that they already suffer. The model explains more than 85% of the variance of all disease incidents in the



Content from this work may be used under the terms of the [Creative Commons Attribution 3.0 licence](https://creativecommons.org/licenses/by/3.0/). Any further distribution of this work must maintain attribution to the author(s) and the title of the work, journal citation and DOI.

population. The presented methodology could be of importance for anticipating age-dependent disease profiles for entire populations, and for design and validation of prevention strategies.

 Online supplementary data available from stacks.iop.org/njp/16/115013/mmedia

Keywords: network medicine, disease dynamics, multilayer statistics, medical claims data

1. Introduction

Diseases are usually defined by a set of phenotypes that are associated with various pathobiological processes and their mutual interactions. Recently, there has been impressive progress in the understanding of various types of relations between disease phenotypes on the basis of common underlying molecular processes [1]. For example, two diseases can be related if there are genes that are associated to both of them [2–5]. It was shown that genes associated with the same disorder encode proteins that have a strong tendency to interact with each other [2]. Alternatively, one can think of two diseases being linked and related if their metabolic reactions within a cell share common enzymes [6]. Networks of protein–protein interactions [7, 8] have also been studied in the context of disease interactions [9, 10]. Such interaction networks for seemingly unrelated gene products were shown to be involved in a group of different diseases that share clinical and pathological phenotypes [10].

The large number of relations between myriads of cellular components implies that diseases are not a clearcut concept, but merely act as some sort of a ‘discretization’ in a vast and complicated phenotype space [1]. The structure of this space is typically studied through phenotypic comorbidity relations between human diseases. A comorbidity relation means that two diseases occur more frequently within a patient than what would be expected from the frequency of the individual diseases alone. This means that the joint probability for suffering two diseases i and j together is larger than the product of the probabilities of the individual diseases (prevalences), $P(i, j) > P(i)P(j)$. A phenotypic human disease network (PHDN) consists of nodes representing the diseases and links that indicate comorbidity relations [11]. PHDNs have opened a novel way for doing medicine on a population-wide scale. For example it has been shown that there exist pronounced ethnic differences in the PHDNs of black and white males [11], and that PHDNs may be used to predict future sites of cancer metastasis [12]. Note that only a limited number of comorbidities can be explained by common genes, proteins, or metabolites [4, 13]. These differences with respect to the clinical reality of disease not only reflect our limited knowledge of cellular processes, they also underscore the role of environmental and epigenetic factors in disease progression. Another class of highly relevant networks in medicine are physiological networks that describe interactions of organ systems in the human organism [14, 15]. Changes in physiological function can be understood as topological transitions of such physiological networks [14, 15].

The age-dependence of PHDNs is hitherto unknown. Up to now, studies on US Medicare data have uncovered comorbidity relations in patients aged 65 and older [11, 13]. In this work we use a complete medical claims data set that contains information on all of the 8.3 million

Austrians who received medical treatments in the years 2006 and 2007. The data set has been studied before to show a strong relationship between hunger in early life and the development of metabolic diseases in later life [16, 17]. Further, the nationwide age and gender dependence of diabetic complications was studied on the same data set [18].

For the first time, here we obtain a specific age-dependent PHDN of all statistically significant comorbidity relations that pose a substantial risk to male or female patients. We do so by proposing a new statistical method that leads to an age- and genderspecific disease–disease network. This network is obtained by combining the layers of a disease–disease multiplex network that consists of two layers that encode different phenomenological statistical measures for disease–disease relations. In the first layer links quantify the statistical significance of a comorbidity relation between two diseases through their correlation coefficient for binary data. The technical challenge here is that the prevalences of individual diseases can vary over several orders of magnitude, from affecting a few dozens to ten thousands of patients in the database [11]. This variability leads to biases in the correlations [19]. In particular, correlations between highly frequent and rare diseases tend to be underestimated [11, 19]. We therefore employ a multi-scale correction that accounts for this bias [20]. Links between nodes i and j in the second layer represent the risk of obtaining disease i , given that the patient already suffers from disease j . The first layer encodes information whether there exists a significant relation between two diseases; the second layer quantifies the risk that a disease relation poses to the patient.

We quantify the topological network properties of the so-obtained PHDN and show that they undergo massive structural and gender-specific changes across lifetime. We show that this analysis allows us to understand the progression of the health state of a population on a new level. Various stages of life are characterized by a unique combination of tightly interrelated disease clusters. With changing patient age, these clusters of diseases emerge, vanish, merge, or form local hubs. To a certain degree the concept of individual diseases becomes meaningless; what determines disease risks and the health state of a population more effectively is the strongly age-dependent mesoscopic organization of the PHDN in disease clusters.

Finally, we develop a simple network diffusion model for the population-wide dynamics of disease progressions. The model is based on the empirical age- and gender-specific comorbidity relations recorded in the PHDN. In particular, we show that using (i) the prevalence of all diseases within a specific age group and (ii) the age-dependent network structure of diseases for a given age, we can explain more than 85% of the variance of the appearances of new diseases within the next eight years in the total population. These results might provide important information for estimating the future burden of diseases in an aging society. The fraction of the EU population aged 65 or older will almost double by the year 2060 to 29.6% of the population, from 17.5% in 2011. The average age of the EU-27 citizen is estimated to be 47.6 years, compared to 41.2 years in 2011 [21]. However, quality of life is not determined by mere life expectancy *per se*, but by the number of years that are spent in healthy conditions. Healthy-life years differ greatly between men and women and across member states of the EU. Whereas life expectancy for women is 6.4y higher than for men, the number of healthy-life years for women is only 1.2y higher [22]. Aging of the population has severe implications for economic growth. Estimates suggest that by 2030 the EU-27 will experience a 14% decrease in workforce and a 7% decrease in consumer population due to aging [23]. It is therefore one of the big societal challenges to understand and anticipate to what extent the aging of the population will affect the future health state of a population.

2. Data and methods

2.1. Data

We use a database of the Main Association of Austrian Social Security Institutions that contains pseudonymized claims data of all persons receiving outpatient and inpatient care in Austria between 1 January 2006 and 31 December 2007. The data provides a comprehensive, nationwide collection of the medical condition of the vast majority of Austria's population of 8.3 million people. Information on diagnoses is available for all persons receiving inpatient care, so-called inpatients. The total sample of inpatients consists of 1,862,258 patients (1,064,952 females and 797,306 males) and includes their year of birth, gender, date of death, their drug prescriptions, and main- and side-diagnoses. Patients are grouped according to their age. The age groups, labeled by a , contain all patients whose age is between a and $a + 8$ years. Diagnosis are provided in the 10th revision of the International Statistical Classification of Diseases and Related Health Problems (ICD 10) [24], a medical classification list by the World Health Organization (WHO). Not all ICD codes represent disorders—they may also indicate general examinations, injuries, pregnancies, or collections of symptoms that could be indicative of a large number of diseases. We exclude these categories and work with the $D = 1,055$ diagnoses on the three-digit ICD levels in chapters A – N . We will use the words disease, disorder, and diagnosis interchangeably whenever referring to a specific ICD entry. It was found that such data can generally be considered to be complete with only a small amount of gross diagnostic miscoding [25]. Prognostic models for hospitalizations built on comorbidity scores derived from medical claims data perform similarly well as survey-derived data [26].

2.2. Derivation of the disease network from a statistical multiplex network

We use the following notation. In our data we have $N^{m/f}(a)$ men/women in age group a . Let us consider index pairs, where index i indicates patients suffering disease i and $\neg i$ indicates patients not having the diagnosis i . Each of the $N^{m/f}(a)$ patients belongs to one of four index pairs, $\{(i, j), (\neg i, j), (i, \neg j), (\neg i, \neg j)\}$, meaning that the patient has diseases i and j , has j but not i , has i but not j , or has neither i nor j , respectively. The numbers $N_{i,j}^{m/f}(a)$, $N_{i,\neg j}^{m/f}(a)$, $N_{\neg i,j}^{m/f}(a)$, $N_{\neg i,\neg j}^{m/f}(a)$ denote the number of male/female patients in age group a in these respective groups. The *prevalence* for each disease i is defined as $p_i^{m/f}(a) = \frac{N_i^{m/f}(a)}{N^{m/f}(a)}$. In the following, we sometimes suppress the indices for age and gender for clarity.

2.2.1. Layer 1: statistical significance of comorbidity relations. The first layer of the PHDN multiplex provides the statistical significance of relations between any two diseases i and j . With the above notation the contingency coefficient ϕ_{ij} for a specific age group is defined by

$$\phi_{ij} = \frac{N_{i,j}N_{\neg i,\neg j} - N_{i,\neg j}N_{\neg i,j}}{\sqrt{N_i N_{\neg i} N_j N_{\neg j}}}. \quad (1)$$

A value of $\phi_{ij}(a)$ is computed for the patient numbers in each age group a . These values are directly related to the chi-square-coefficient $(\chi_{ij})^2(a) = N(a)(\phi_{ij}(a))^2$, where $N(a)$ is the number of patients in the considered age group. A chi-square test can be used to reject the null hypothesis for a given confidence level that the occurrence of disease i is independent of the

occurrence of disease j in the same patient. $\phi = (\phi_{ij})$ is a symmetric matrix containing the test statistics for diseases i and j . We discard negative entries by setting $\phi_{ij} \rightarrow 0$, whenever $\phi_{ij} < 0$. For later use we define an unweighted adjacency matrix J derived from ϕ by defining $J_{ij} = 1$ if $\phi_{ij} > 0$, and $J_{ij} = 0$ otherwise.

There are known biases in the test statistic ϕ_{ij} that depend on the prevalences $p_i^{m/f}(a)$ and $p_j^{m/f}(a)$ of the diseases i and j . While the contingency coefficient is a reliable measure for correlations whenever diseases i and j have similar prevalences $p_i^{m/f}(a)$ and $p_j^{m/f}(a)$, ϕ underestimates correlations between very rare and highly frequent diseases [11, 19]. It is therefore unclear if low values for ϕ_{ij} for two diseases i and j imply weak correlations or large differences in their respective prevalences.

Assume that disease i has a very low prevalence $p_i^{m/f}(a)$ with respect to the prevalence values of the majority of other diseases. Then each of its ϕ -values can be assumed to underestimate the true correlations, with respect to similar ϕ -values obtained from more frequent diseases. A simple way to correct these biases is to compare values of ϕ_{ij} for disease i with the typical correlation strength for disease i [20]. To this end, consider the matrix

$$\tilde{\phi}_{ij} = \frac{\phi_{ij}}{\langle \phi \rangle_i}, \quad (2)$$

where $\langle \phi \rangle_i = \frac{\sum_{j=1}^D \phi_{ij}}{\sum_{j=1}^D J_{ij}}$. While ϕ is an undirected network, $\tilde{\phi}$ is typically directed. To obtain a unique and bias-corrected measure for the strength of the correlation between diseases i and j , an undirected version ϕ^* of the network $\tilde{\phi}_{ij}$ is obtained by $\phi_{ij}^* = \max \{ \tilde{\phi}_{ij}, \tilde{\phi}_{ji} \}$.

2.2.2. Layer 2: conditional disease risk. The second layer of the PHDN multiplex is given by the risk for a patient of a certain age group and gender to have disease i , given that she has disease j . The conditional probability $P(i|j)$ for a patient who suffers disease j to also suffer disease i is given by $P(i|j) = \frac{N_{ij}}{N_j}$. A thresholded, undirected, and unweighted version P^* of $P(i|j)$ is

$$P_{ij}^* = \begin{cases} 1 & \max \{ P_{ij}, P_{ji} \} > p_c, \\ 0 & \text{otherwise} \end{cases}, \quad (3)$$

for a given threshold $p_c > 0$.

2.2.3. Overlap of the multiplex network layers. The overlap (intersection) of the two multiplex network layers, ϕ^* and P^* , the network O , is given by

$$O_{i,j} = \begin{cases} 1 & \text{if } \phi_{ij}^* > \phi_c \text{ and } P_{ij}^* > p_c. \\ 0 & \text{otherwise} \end{cases}. \quad (4)$$

The network O_{ij} links two diseases i and j if the link weights in both network layers exceed given thresholds—namely, ϕ_c for the statistical significance layer Φ^* , and p_c for the conditional risk layer P^* . Note that up to first order of $\frac{1}{\sum_{j=1}^D J_{ij}}$ the thresholding of the statistical significance

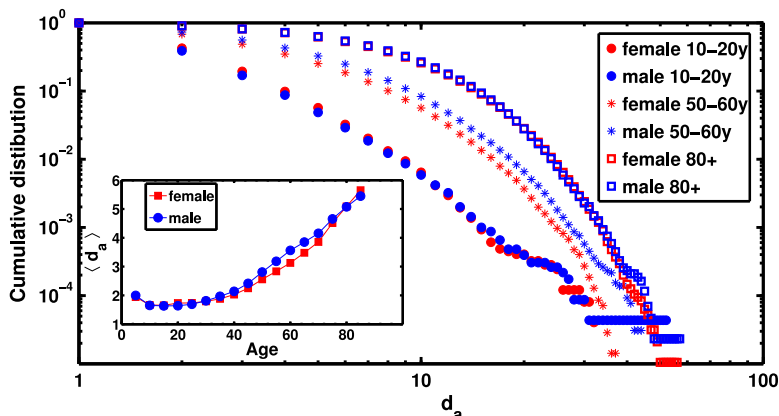


Figure 1. Cumulative distributions of the number of diagnoses for a typical inpatient for three age groups $a = 10\text{--}20$ years, $50\text{--}60$ years, and $a > 80$ years are shown. In the first age group the disease distributions follow an approximate power-law. In older ages the distributions look more exponential. The inset shows the average number of diagnoses $\langle d_a \rangle$ for inpatients for women (red squares) and men (blue circles). Standard deviations of d_a are smaller than the symbol size.

layer ϕ^* by the value ϕ_c , as done in equation (4), yields the same results as the application of the multiscale filter proposed in [20]. From now on we refer to O_{ij} simply as the ‘disease network.’ It is a variant of a PHDN. In contrast to the PHDN studied in [11], the disease network O_{ij} is built around a combination of measures (conditional probabilities and contingency coefficients) that have been corrected for biases that result from the comparison of very rare and frequent diseases.

3. Results

3.1. Progression of diseases with aging

Let d_a be the number of diseases diagnosed in patients with a hospital stay of at least one day in a given age group during the two years 2006 and 2007. Figure 1 shows the cumulative distribution functions (cdf) for the numbers of diseases d_a for three different age groups, $a = 10\text{--}20$ years, $a = 50\text{--}60$ years, and $a > 80$ years, for males and females. The cdf for all age groups are presented in supplementary information (SI) figures 1 and 2. In the first age group the distribution suggests an approximate power-law behavior up to about 20 diseases. With increasing age the disease distributions takes on a more exponential character. The average number of diseases per patient in each age group, $\langle d_a \rangle$, is shown in the inset of figure 1. Children in the first age group have a higher average number of diagnoses than teenagers. After adolescence there is a continuous increase in the number of diseases per patient in the population, from two (at the age of around 20) to more than five for patients older than 80. Men between 30 and 70 have generally more diseases than women, which reverses at older ages. The number of diagnoses for females around 20 is higher than those for males.

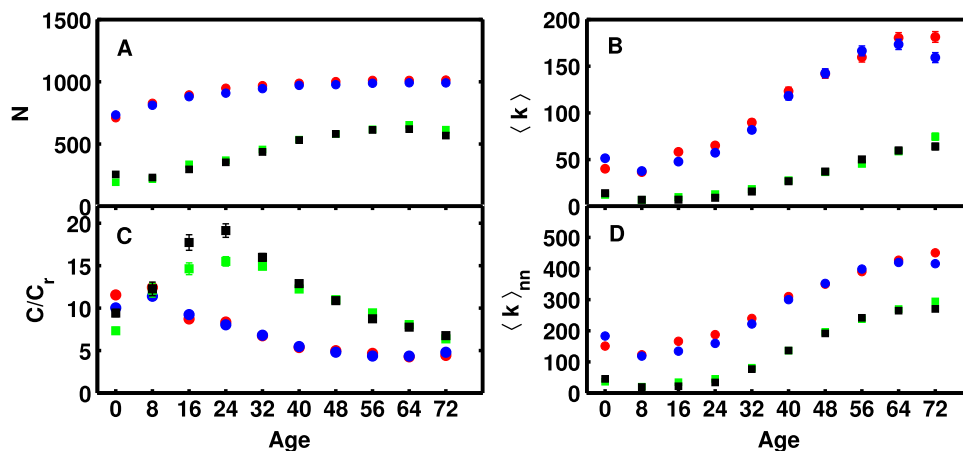


Figure 2. Basic network properties for the two levels P^* and ϕ^* of the multiplex are compared across age. Results for the conditional risk layer are shown in circles for females (red) and males (blue). For the statistical significance layer ϕ^* results are shown for females (green) and males (black) in squares. (A) The number of nodes N with at least one link increases in both network layers from childhood into adulthood and levels off at higher ages. (B) Average degrees $\langle k \rangle$ increase over age. (C) Values of the clustering coefficients C divided by C_r (clustering coefficient for corresponding random graph) show a pronounced peak around age 25 for the ϕ^* network, and a consistent decrease in clustering for P^* . (D) Average degrees of nearest neighbors $\langle k \rangle_{nn}$ increase with age. Error bars show the standard deviations.

3.2. Network properties of the disease network

The large increase in diagnoses per patient over age is related to substantial topological changes of the ϕ^* and P^* networks. Network properties for the two layers are shown in figure 2. The number of nodes N (figure 2(A)), the average degrees $\langle k \rangle$ (figure 2(B)), and the average nearest neighbour degrees $\langle k \rangle_{nn}$ (figure 2(D)), increase with age in both layers. For patients aged above 65 the degrees are larger for women than for men. The clustering coefficients C for each network are given in units of the clustering as expected from a random graph, C_r , in figure 2(C). C/C_r is larger for ϕ than for the conditional risk layer for all age groups except for the youngest children. This ratio shows a clear maximum around age 25 in the ϕ^* layer, but it decreases monotonically in the P^* layer. Correlation coefficients between the degree sequences of ϕ^* and P^* are given for two choices of thresholds in the SI; see table S1. In one case we set the thresholds in the ϕ^* and P^* layers to $p_c = 0.01$ and $\phi_c = 2$, respectively, and in the other case the thresholds are both zero, $p_c = \phi_c = 0$. We find higher degree correlations across the two layers for the non-zero threshold values, compared to the case where the thresholds are both zero. This suggests that the thresholding tends to filter out links that appear in only one of the layers. With increasing patient age, the difference between the degree correlations also increases.

Network properties for the disease network O for the threshold values $\phi_c = 2$ and $p_c = 0.01$ are shown in figure 3. The numbers of nodes N (figure 3(A)), average degrees $\langle k \rangle$ (figure 3(B)), and the ratios of clustering coefficients C/C_r (figure 3(C)), show a similar behavior with increasing age. They decrease from the first to second age group, and increase until about age 50. For higher ages the increase levels off and the network measures decrease again. The

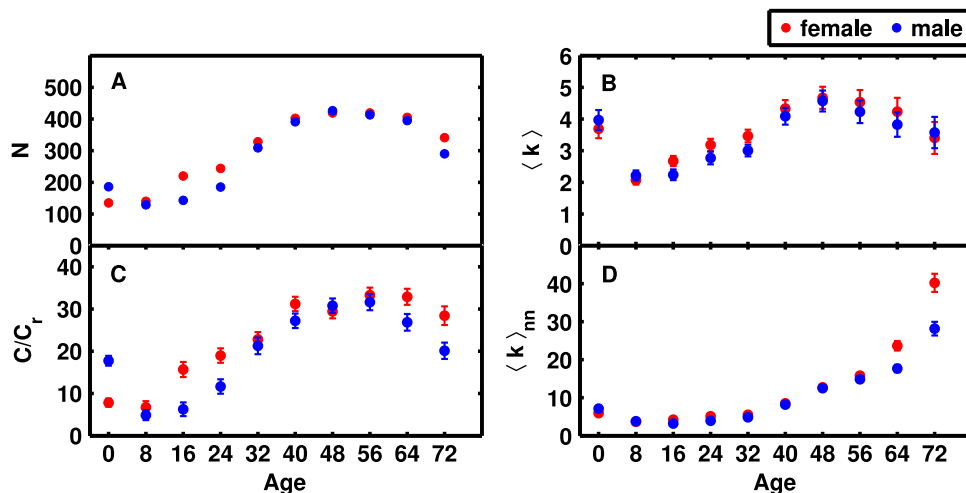


Figure 3. Network properties for the disease network O . (A) number of nodes N , (B) average degree $\langle k \rangle$, (C) clustering coefficients in units of C_r , and (D) average nearest neighbor degrees $\langle k \rangle_{nn}$. O has the highest density for males and females aged 48–56. Children are characterized by a higher density and higher clustering than teenagers. There is a subsequent increase in N , $\langle k \rangle$, and C/C_r with age, up to a maximum value at around age 50. The average degree of the nearest neighbors $\langle k \rangle_{nn}$ increases also for older ages. Error bars show the standard deviations.

average nearest neighbour degrees do not level off at high ages but continue to increase; see figure 3(D). The disease network is most dense for both males and females for the age range 48–56. Results for the modularities of ϕ^* , P^* , and O as a function of patient age and gender are shown in the SI; see figure S6. The disease network O has typically higher modularities than the layers ϕ^* and P^* , which suggests that disease clusters can be easier identified in O than in its individual layers. We confirmed that the network properties shown in figure 3 are to a large extent independent from the actual choices of the threshold values p_c and ϕ_c ; see SI figures S7–10.

Visualizations of the disease networks O across lifetime are presented in figure 4 for males and females. Massive structural reorganization in the disease networks are clearly visible across age. Nodes represent diseases i ; their size is proportional to the disease prevalence, $N_i^{m/f}(a)$. The diseases type, as represented by the first letters from the ICD 10 code, is indicated by node colors. Link colors are identical to the node colors if both diseases share the same type; otherwise, it is a mix of the two colors. Disease clusters belonging to the same ICD type (first letter of ICD code) are highlighted by colored patches in figure 4. Alternative visualizations of the disease networks O are shown in the SI, figures S21–28, for each age group and gender. In figures S21–28 we set $p_c = 0.02$ and adjust ϕ_c such that each network has the same average degree $\langle k \rangle$.

3.3. Evolution of the human disease network across lifetime

We find three distinct phases in the evolution of the diseases networks across lifetime.

Phase I. The disease network for children, phase I (age 0–16), shows one cluster containing diseases of many different types, such as diseases of the respiratory system (letter J

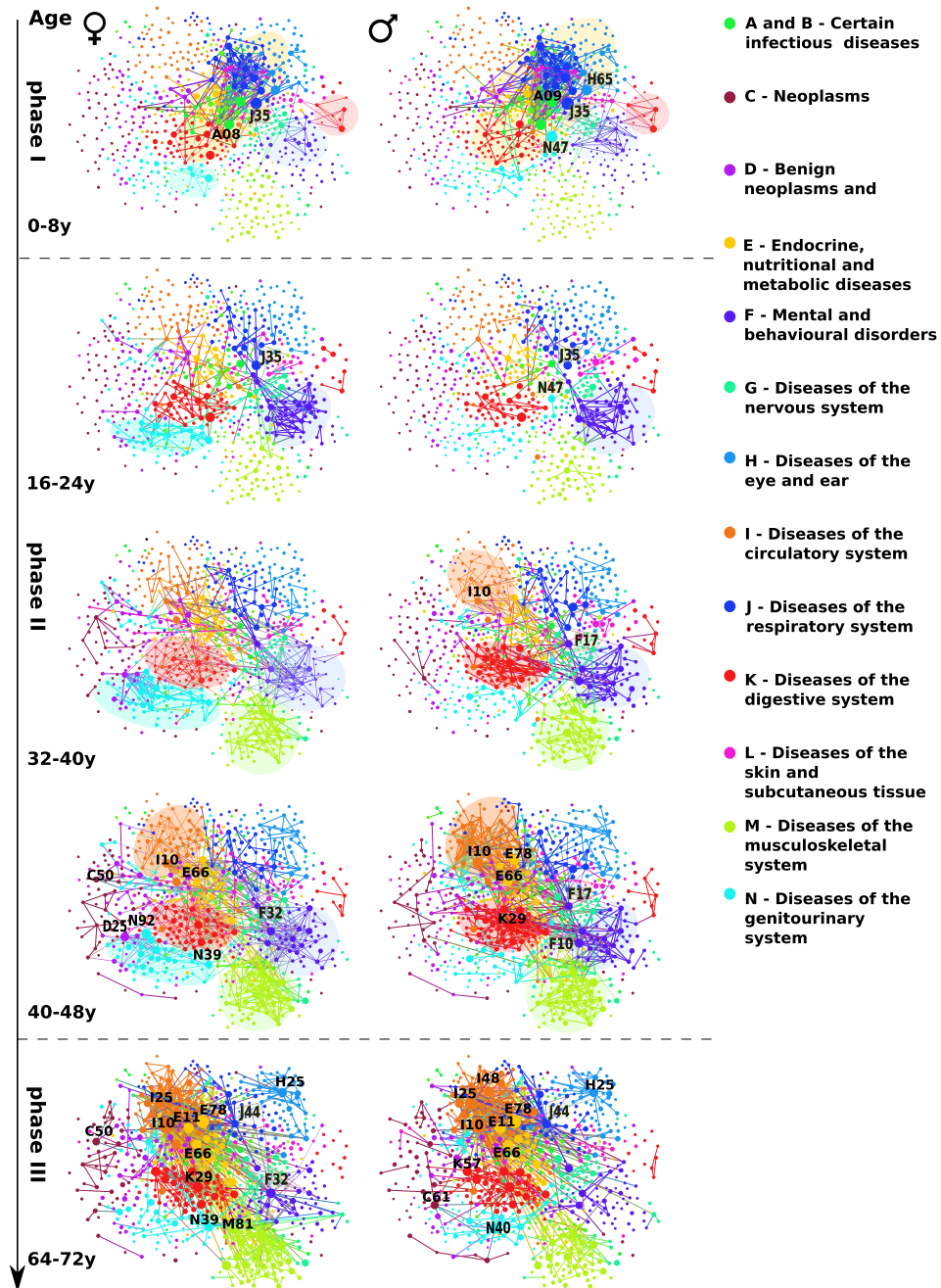


Figure 4. Evolution of the disease network for females (left) and males (right). Each network corresponds to a snapshot at a given age, with age increasing from top to bottom. Node sizes represent disease prevalences; the colors indicate the main classifications of diseases according to the first letter of the ICD 10 codes. The evolution of the disease network proceeds in roughly three phases: *phase I*, children’s diseases, characterized by one large cluster and several small ones. *Phase II*, adult groups, in which many different and clearly distinguishable clusters appear. *Phase III*, the network for elderly patients, where the network becomes increasingly dominated by hubs. Colored patches serve as guides to the eye for clusters of diseases belonging to the same type.

in the ICD code), infectious diseases (A), diseases of the eye and ear (H), and endocrine, nutritional, and metabolic diseases (E). Highly prevalent are viral and other specified intestinal infections (A08), diarrhea and gastroenteritis of presumed infectious origin (A09), chronic diseases of tonsils and adenoids (J35), and non-suppurative otitis media (H65). These diseases correspond to nodes that are characterized by large degrees and tend to be connected to each other. There is a small cluster formed by diseases of the nervous system (G), with a local hub being epilepsy (G40), and a cluster for mental and behavioral disorders (F). For male children there is a cluster containing disorders of psychological development that is not visible for females. For females in phase I there are small clusters containing diseases of the digestive system (K) and of the genitourinary system (N), whereas for males phimosis and paraphimosis (N47) belong to the main cluster. The network for young males is in general more dense than for females in phase I, but the formation of disease clusters and the prevalences are similar. The network for patients aged 8–16 is less dense than the network of the former age group, but the same clusters are still visible (see SI figure S12). There are obvious changes, however, for the next age group, 16–24, (see figure 4, second row), where the cluster for mental diseases (F) dominates and contains more different nodes than in the previous networks. This can be seen as the onset of the structural phase II of the disease networks.

Phase II. In phase II (age 16–64), a cluster of mental and behavioral disorders (F) appears more clearly and contains addiction to nicotine, alcohol, and other substance abuses. It has a higher density for women than for men. For both genders in the age group 16–24, the prevalences of diseases are smaller than in phase I, but infections (A08 and A09), tonsil problems (J35), and disorders of the prepuce for men (N47) are still highly prevalent. Children and young patients suffer similarly from obesity (E66), which becomes increasingly prevalent starting with patients aged 16–24y. Hypertension (I10) becomes also visible at this age, but it is not yet a dominant disease.

At ages 32–40 the cluster of diseases of the digestive system (K) emerges for men (see figure 4, third row). Hemorrhoids (I84) are found at the periphery of this cluster with links exclusively to digestive diseases; there are no links from hemorrhoids to any other circulatory disease. The cluster of diseases of the genitourinary system (N) exists still only for women and grows with age. It is connected to benign neoplasms and blood diseases (D). For patients over 40, leiomyoma of the uterus (D25) are very common. This disease has many links to both genitourinary disorders (N) and to malignant neoplasms (C), especially related to female genital organs. The most prevalent neoplasms are breast cancer (C50) for women and prostate cancer (C61) for men. Neoplasms are located at the periphery of the network and show many inter-cluster connections, such as links to secondary neoplasms.

The cluster of circulatory diseases (I) appears for men older than 32 and women older than 40. It densifies for older age groups. This cluster is also much denser for men than for women; see figure 4, fourth row. Another gender difference for this age group is the absence of genitourinary diseases (N) for men, while for women these diseases become increasingly prevalent until the age of 40. The most common circulatory disease is hypertension (I10). Already at age 40–48 it has a large number of links inside and outside the cluster of circulatory diseases.

The origin of the cluster related to diseases of the musculoskeletal system (M) is visible for both genders at age 24–32 (see SI figure S14); for older groups, this cluster becomes denser more quickly for females than for males. This may be related to osteoporosis (M81), which is a hub only for women over 48 and serves as a gateway to many musculoskeletal diseases. An

important structural change begins at age 64, where some clusters start to shrink, such as mental disorders (F) and genitourinary diseases (N) for women. This marks the beginning of phase III (age 64–80) of the evolution of the disease network.

Phase III. A contraction of the network toward its center can be observed in figure 4, bottom row, where it becomes increasingly dominated by circulatory (I) and metabolic (E) diseases. Global hubs appear—in particular, hypertension (I10), depression (F32), ischemic heart diseases (I25), chronic obstructive pulmonary disease (COPD, J44), the metabolic syndrome including disorders of lipoprotein metabolism (E78), type 2 diabetes (E11), and obesity (E66). There are also some local hubs—for example, cataracts (H25). Clearly discernible clusters disappear in phase III, with the exception of musculoskeletal disorders (M) for females. Neoplasms (C) become increasingly interconnected. The effect of the network contraction progresses in the oldest groups (age 72–80), where it is even more difficult to distinguish specific clusters (see SI figure S19).

The three phases are also apparent in the evolution of the network properties of the disease network; see figure 3. In phase I (childhood) we find large clustering and degrees at a comparably small network size N . This suggests a tightly interconnected cluster of diseases spanning only a small part of the entire possible network. Phase II presents itself as a steady increase in clustering and network density. This trend levels off once substantial parts of the network show high levels of disease prevalences. In phase III clustering and density decrease, whereas the average nearest neighbor degree increases. This suggests the emergence of hubs that become connected to an increasing number of other diseases, whereas the local clusters that characterize phase II disappear. On a more quantitative level, we fitted the degree distributions with q -exponentials [27, 28] and report the values of q for males and females across age groups in figures S2–4 in the SI. In general, q increases over lifetime, but there is a prominent peak at ages 16 and 24, indicating again a massive change of regime in network topology.

4. Network diffusion model of disease progression on the population level

It has been suggested that the spread of diseases may be related to a diffusion process on disease networks [11]. Along these lines we propose a simple model that assumes that individuals can acquire new diseases that are comorbidities of already existing ones. This is, of course, a crude simplification of the actual processes that lead to disease incidences.

Assume that the prevalence of disease i in males/females of age group a is $p_i^{m/f}(a) = \frac{N_i^{m/f}(a)}{N^{m/f}(a)}$. Let the expected prevalence of disease i at the next age group be denoted by $\hat{p}_i^{m/f}(a+1)$. We then make the simple network diffusion Ansatz,

$$\hat{p}_i^{m/f}(a+1) = p_i^{m/f}(a) + (1 - p_i^{m/f}(a)) \sum_{j \neq i} \Delta P_{ij}^{m/f}(a) p_j^{m/f}(a), \quad (5)$$

where $\Delta P_{ij}^{m/f}(a) = P_{ij}^{m/f}(a+1) - P_{ij}^{m/f}(a)$ is the difference between the conditional disease risks for age groups $a+1$ and a . $\Delta P_{ij}^{m/f}(a)$ is the risk of obtaining disease i given j for a patient aging from age group a to $a+1$. This number is multiplied with the probabilities to have disease j and to *not* have disease i to give the disease network effect on the disease prevalences.

To estimate the quality of the model, we compute the correlation coefficient ρ between the actually observed prevalences at the next timestep, $p_i^{m/f}(a+1)$, and the predicted result of

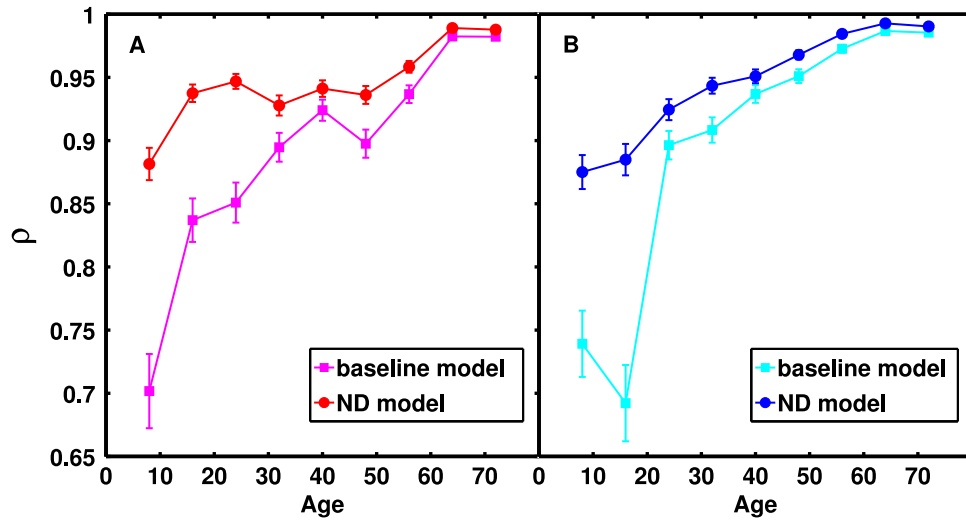


Figure 5. Correlation coefficients ρ between actual prevalence data and predictions from the network diffusion model (NDM) are shown for females (A) and males (B). NDM results are compared to the baseline model without diffusion term. The disease network effect (difference between lines) consistently increases correlations by up to 20%, especially for children and adolescents. The importance of diffusion diminishes with higher ages.

equation (5), $\rho = \text{corr}(\hat{p}_i^{m/f}(a+1), p_i^{m/f}(a+1))$. The value of ρ quantifies how much of the variance of disease prevalences at a given age a can be explained by the prevalences of diseases in the previous age group, superimposed by the risk from disease spreading from nearby nodes in the disease network. The values for ρ for the network diffusion model (NDM) are shown in figure 5(A) for women and figure 5(B) for men. The correlation coefficients for the NDM are higher than 90% for ages above 50. To estimate the importance of comorbidities in the NDM, we compare its results with the correlation coefficient obtained for a variant of the model in equation (5), where we ignore the second term on the right-hand side; i.e., we ignore effects from the disease network and set $\Delta P_{ij}^{m/f} = 0$. This variant we call the ‘baseline model.’ Results are also collected in figure 5. These results suggest that a substantial fraction of disease incidents can be predicted on the basis of the diseases that exist at the previous age group alone. Clearly, the diffusion model consistently outperforms the baseline model for all ages and gender groups. In the age range 40–80 the disease network effect increases the explanatory power compared to the baseline model only by a couple of percentage points. Gender differences can be observed. For women at age 48 the quality gap between the models is about 5%, compared to 2–3% for men. This may be related to physiological changes during the menopause. Important physiological changes also take place during puberty and adolescence. During these ages the baseline model is able to explain up to 70% of the variance of disease prevalences, whereas the NDM performs substantially better 85–90%.

5. Discussion

The health state of patients is typically characterized by multiple comorbid conditions, especially among adults and the elderly. We proposed a phenotypic human disease network that

is derived from a multiplex network of two statistical measures quantifying relations between diseases. This network contains information about which diseases are typically treated together in a patient. We showed that the disease network undergoes dramatic structural transformations as a function of patient age and gender. In particular, one can distinguish three phases in the evolution of the disease network. The first phase describes the comorbidity relations in children and consists of a single, strongly interconnected cluster. The second phase for adolescents and adults is characterized by the appearance of subsequent clusters related to specific classes of diseases. For instance, clusters of mental disorders appear in both genders in younger adults, whereas genitourinary disorders appear only for women. Clusters for circulatory, musculoskeletal, and digestive diseases appear in subsequent life years. In the last phase, for elderly people above 65, disease clusters condense and several highly connected hubs appear and dominate the network. These hubs are hypertension, chronic ischemic heart diseases, and COPD. Interestingly, it has been shown that several cardiac and respiratory functions undergo abrupt changes at around age 65, where the transition from phase II to III occurs [29, 30]. The results presented here allow us to understand developments in population health across life in a new way. With the adoption of a network perspective, the focus shifts from the study of individual disease progression to transformations of the mesoscopic organization of the disease network. We showed that each stage of life can be characterized by its unique set of clusters of closely interrelated diseases.

We developed a network diffusion model that shows that patients indeed develop new diseases in close proximity in the disease network to disorders they already have. A thorough topological understanding of disease–disease relations is therefore key to anticipating future developments in population health. It is remarkable that the vast majority of new disease onsets can be explained by the conditional disease risks $P(i|j)$ alone. Combined with models that describe demographic changes in the age structure of a population, the network diffusion model proposed in this work may provide an attractive starting point to predict future burdens of diseases within an aging society.

Acknowledgments

AC was supported by the EU FP7 project LASAGNE no. 318132, PK by EU FP7 project MULTIPLEX No. 317532.

References

- [1] Barabási A-L, Gulbahce N and Loscalzo J 2011 *Nat. Rev. Genet.* **12** 56–68
- [2] Goh K-I, Cusick M E, Valle D, Childs B, Vidal M and Barabási A-L 2007 *Proc. Natl Acad. Sci.* **104** 8685–90
- [3] Feldman I, Rzhetsky A and Vitkup D 2008 *Proc. Natl Acad. Sci.* **105** 4323–8
- [4] Rzhetsky A, Wajngurt D, Park N and Zheng T 2007 *Proc. Natl Acad. Sci.* **104** 11693–9
- [5] Park J, Lee D S, Christakis N A and Barabási A-L 2009 *Mol. Syst. Biol.* **5** 1–7
- [6] Lee D S, Park J, Kay K A, Christakis N A, Oltvai Z N and Barabási A-L 2008 *Proc. Natl Acad. Sci.* **105** 9880–5
- [7] Jeong H, Tombor B, Albert R, Oltvai Z N and Barabási A-L 2000 *Nature* **407** 651–4
- [8] Jeong H, Mason S P, Barabási A-L and Oltvai Z N 2001 *Nature* **411** 41–2
- [9] Ideker T and Sharan R 2008 *Genome Res.* **18** 644–52
- [10] Lim J *et al* 2006 *Cell* **125** 801–14

- [11] Hidalgo C A, Blumm N, Barabási A-L and Christakis N A 2009 *PLoS Comput. Biol.* **5** 1–11
- [12] Chen L L, Blumm N, Christakis N A, Barabási A-L and Deisboeck T S 2009 *Br. J. Cancer* **101** 749–58
- [13] Davis D A and Chawla N V 2011 *PLoS One* **6** e.22670
- [14] Bashan A, Bartsch R P, Kantelhardt J W, Havlin S and Ivanov P C 2012 *Nat. Commun.* **3** 702
- [15] Bartsch R P and Ivanov P C 2014 *Nonlinear Dynamics of Electronic Systems, Communications in Computer and Information Science* vol 438 (Berlin: Springer) pp 270–87
- [16] Thurner S, Klimek P, Szell M, Duftschmid G, Endel G, Kautzky-Willer A and Kasper D C 2013 *Proc. Natl Acad. Sci.* **110** 4703–07
- [17] Klimek P, Leitner M, Kautzky-Willer A and Thurner S 2014 *Gerontology* **60** 502–7
- [18] Klimek P, Kautzky-Willer A, Chmiel A, Schiller-Frühwirth I and Thurner S arXiv:1310.7505
- [19] Olivier J and Bell M L 2013 *PLoS One* **8** e58777
- [20] Serrano M A, Boguna M and Vespignani A 2008 *Proc. Natl Acad. Sci.* **106** 6483–8
- [21] EUROPOP2010—Convergence scenario, national level (Eurostat, Luxembourg, 2011)
- [22] EHLEIS Country Reports Issue 6 (EHLEIS Technical Report 20134.1, 2013)
- [23] Hewitt P S, Depopulation and aging in Europe and Japan: The hazardous transition to a labor shortage economy. International Politics and Society, January 2002.
- [24] <http://apps.who.int/classifications/icd10/browse/2010/en>, retrieved 05/03/2014
- [25] Hennessy S, Leonard C E, Palumbo C M, Newcomb C and Bilker W B 2007 *Med. Care* **45** 1216–20
- [26] Zhang J X, Iwashyna T J and Christakis N A 1999 *Med. Care* **37** 1128–39
- [27] Thurner S and Tsallis C 2005 *Europhys. Lett.* **72** 197–203
- [28] Thurner S, Kyriakopoulos S and Tsallis C 2007 *Phys. Rev. E* **76** 036111
- [29] Schumann A Y, Bartsch R P, Penzel T, Ivanov P C and Kantelhardt J W 2010 *Sleep* **33** 943–55
- [30] Schmitt D T, Stein P K and Ivanov P C 2009 *IEEE Trans. Biomed. Eng.* **56** 1564–73